

Anomalous Hall Effect below the Magnetic-Field-Induced Metal-Insulator Transition in Narrow-Gap Semiconductors

V. J. Goldman and M. Shayegan

Department of Electrical Engineering, Princeton University, Princeton, New Jersey 08544

and

H. D. Drew

Department of Physics and Astronomy, University of Maryland, College Park, Maryland 20742

(Received 10 March 1986)

A model is presented in which a semiconductor crystal contains an infinite metallic donor cluster as well as shallow donors which do not have close neighbors thus supporting effectively localized electronic states. The average carrier concentration in the infinite cluster is greater than the crystal-average electron concentration. The model is applied to the Hall effect below the magnetic-field-induced metal-insulator transition in $\text{Hg}_{1-x}\text{Cd}_x\text{Te}$ and InSb .

PACS numbers: 71.30.+h, 72.20.Fr

The metal-insulator (MI) transition in doped semiconductors has been studied for many years^{1,2}; however, our understanding of this phenomenon is far from being complete. Early contributions by Mott and Anderson emphasized the importance of electron correlations and disorder, respectively. The concepts of the mobility edge and smooth potential fluctuations have proved to be fruitful in the pictures of the MI transition in amorphous semiconductors and two-dimensional electron systems.³

The nature of the disorder is, however, different in crystalline semiconductors doped with shallow (hydrogenic) impurities. At high impurity concentrations, such that $a^*n^{1/3} \gg 1$, where n is the electron concentration and a^* is the effective donor Bohr radius, the interaction energy between the conduction-band electrons and the ionized impurities E_i is of the order $e^2n^{1/3}/\kappa$, where κ is the static dielectric constant of the crystal. On the other hand, the Fermi energy is $E_F \sim \hbar^2n^{2/3}/m^*$, where m^* is the conduction-band effective mass. Therefore, at such impurity concentrations $E_i/E_F \sim (a^*n^{1/3})^{-1} \ll 1$, and the electrons can be treated as a nearly ideal gas.⁴ Closer to the MI transition, however, the screening is not effective and the electron-impurity interaction is strong for small separations and cannot be well approximated by a smooth effective potential. In addition, the origin of the disorder in crystalline semiconductors lies chiefly in the randomness of the spatial distribution of shallow impurities and not in the difference in the strengths of the interaction or spatial fluctuations in the band-edge energy.⁵ It is well established that at low impurity concentrations the so-called impurity band is formed¹; however, there is no general agreement on whether the MI transition takes place in the impurity band alone or the hybridized conduction-band states play an important role.³

Although not widely known, there exist several

pieces of direct evidence that the MI transition occurs in the impurity band. Indeed, infrared transmission experiments performed in narrow-gap semiconductors InSb ⁶ and $\text{Hg}_{1-x}\text{Cd}_x\text{Te}$ ⁷ revealed that the absorption due to electronic transitions between donor bound states persists at magnetic fields well below the magnetic-field-induced MI transition. The magnitude of the absorption implies that nearly all donor-band electrons participate in the optical transitions at low temperatures. In another experiment, cyclotron resonance of conduction-band electrons was observed in wide-gap insulating CdSe at liquid helium temperatures under thermal equilibrium conditions.⁸ The origin of the implied extended electronic states was attributed to the MI transition in small clusters of donors of higher than average concentration, resulting from random fluctuations of local donor density.

These experimental results support the tight-binding approach to the donor band in the vicinity of the MI transition. In this paper we present a model based on this approach which we apply to the anomalous Hall effect near, but below, the magnetic-field-induced MI transition in narrow-gap semiconductors.^{9,10} In the absence of magnetic field the samples are metallic. Since the electron effective mass is small it is possible to choose the electron concentrations, leading to the MI transitions' occurring in the strong-magnetic-field limit ($\hbar\omega_c \gg R^*$, where ω_c is the cyclotron frequency and R^* is the effective donor Rydberg constant), thus simplifying the model calculation.

In Fig. 1 plots of the transverse, ρ_{xx} , and Hall, ρ_{xy} , resistivities versus magnetic field are given for a $\text{Hg}_{0.79}\text{Cd}_{0.21}\text{Te}$ sample ($n = 5.4 \times 10^{14} \text{ cm}^{-3}$, $m^* = 0.005m_e$, $\kappa = 17$). The last magnetoquantum oscillation can be seen at $B \approx 0.4 \text{ T}$. At higher magnetic fields only the lowest spin-polarized Landau level is occupied. The MI transition occurs at a field $B_{\text{MI}} \approx 2.0 \text{ T}$. The Hall coefficient $R_H(B) = \rho_{xy}(B)/B$

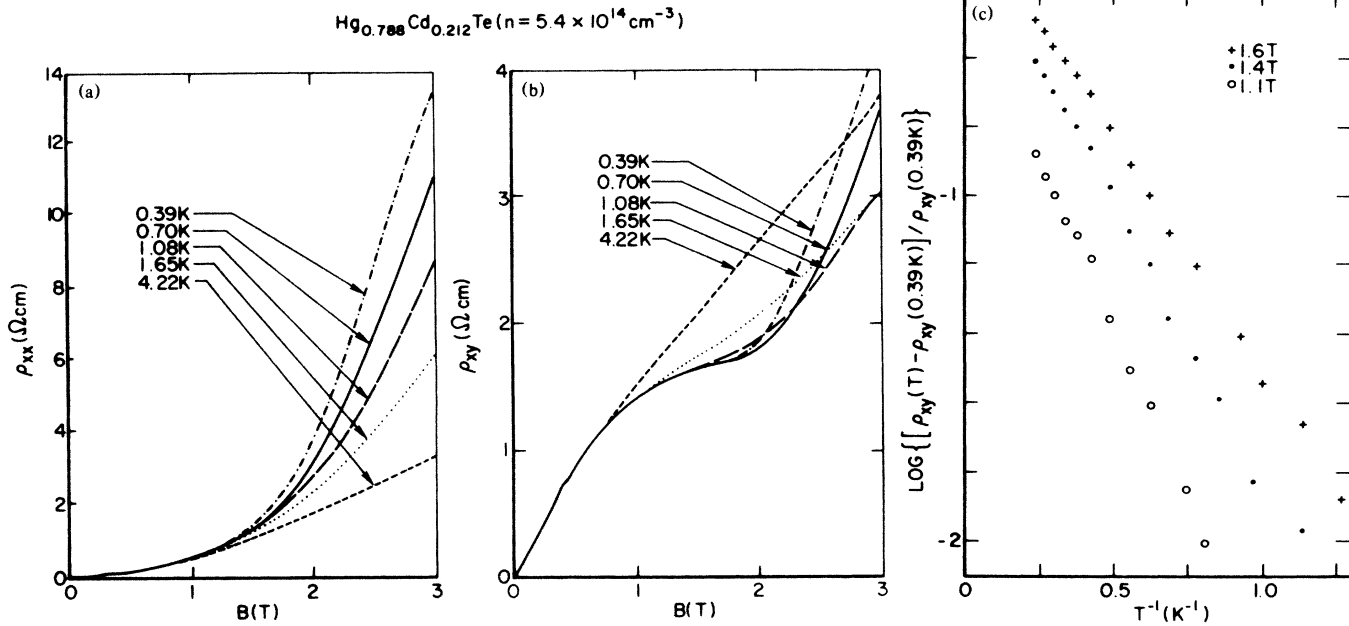


FIG. 1. (a),(b) The transverse, ρ_{xx} , and Hall, ρ_{xy} , resistivities of the $\text{Hg}_{1-x}\text{Cd}_x\text{Te}$ sample ($x=0.212$) as functions of the magnetic field B at several temperatures. The last magnetoquantum oscillation occurs at $B \approx 0.4 \text{ T}$ and $B_{\text{MI}} \approx 2.0 \text{ T}$. (c) The normalized Hall resistivity of the same sample as a function of the inverse temperature T^{-1} at several magnetic fields in the ‘‘Hall dip’’ region (see text).

is shown in Fig. 2 for the same sample at the lowest experimental temperature. At fields below B_{MI} the Hall coefficients of all samples display ‘‘Hall dips,’’^{9,10} i.e., $R_{\text{H}}(B) < R_{\text{H}}(B \rightarrow 0)$ in this region. As the temperature is raised the Hall dip gradually disappears [Fig. 1(c)] and, at $T \sim 10 \text{ K}$, $R_{\text{H}}(B)$ is nearly constant.

In the tight-binding picture the amplitude of the electron wave function peaks on the donor sites and the metallic electrical conduction via the impurity band (in the limit $T \rightarrow 0$) involves tunneling (not hopping) from an occupied to a neighboring unoccupied donor. Still on the metallic side, but not far from the transition, the crystal contains an infinite metallic donor cluster¹¹ as well as regions which do not participate in the electrical transport, i.e., are insulating. For example, a donor which does not have any other donor closer than some distance b supports an effectively localized electronic state¹² for b large enough that the overlap integral of this state with the metallic states is exponentially small. Tunneling through the regions of the crystal containing such a donor is not feasible since it involves large distances.

For randomly placed donors the probability density for a donor to have the nearest neighbor at distance r is given by the Poisson formula

$$P(r) = (r^2/3r_D^3) \exp[-(r/r_D)^3],$$

where $r_D^3 = 3/4\pi N_D$ and N_D is the donor concentration. Therefore, the concentration of the donors

which have no other donor closer than b is

$$\Delta n(b) = \int_b^\infty P(r) dr = n \exp[-(b/r_D)^3]. \quad (1)$$

If we assume that each such isolated occupied donor excludes a volume of $4\pi r^3/3$ from the infinite metallic cluster, the fraction of the volume of the crystal ex-

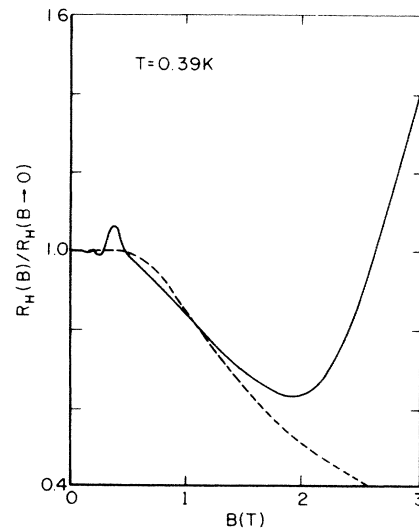


FIG. 2. The normalized Hall coefficient of the sample in Fig. 1 as a function of the magnetic field. The ‘‘Hall dip’’ region extends from the last magnetoquantum oscillation to $B_{\text{MI}} \approx 2.0 \text{ T}$ ($\gamma = 100$). The broken line gives a fit based on Eq. (4) (see text). The fit does not apply for $B \geq B_{\text{MI}}$.

cluded from electrical conduction is

$$\begin{aligned} \epsilon(b) &= n \int_b^\infty (4\pi r^3/3) P(r) dr \\ &= [4\pi b^3/3r_D^3 + 1] \exp[-(b/r_D)^3]. \end{aligned} \quad (2)$$

The conduction takes place in the infinite metallic cluster of the average donor concentration

$$n_{\text{eff}}(b) = [n - \Delta n(b)] / [1 - \epsilon(b)]. \quad (3)$$

Since every isolated donor takes up one electron from the metallic cluster and excludes a volume greater than the average volume per electron, n_{eff} is greater than n . It is known that the Hall coefficient of a macroscopically inhomogeneous material treated within the effective-medium theory is $R_H = h/n_{\text{eff}}e$, where h is a geometrical factor.^{13,14} However, it can be argued that in the case of microscopic inhomogeneities, when electron scattering length is on the order of, or even greater than, the size of typical inhomogeneity, $h \approx 1$.¹⁵

We now apply these results to the narrow-gap semiconductors in a magnetic field. In the strong-field limit, the characteristic size of the electron wave function (for an isolated hydrogenic donor) in the direction parallel to the field is $a_{\parallel}^* = a^*/\ln\gamma$ and perpendicular to the field is $a_{\perp}^* = 2l$, where $l = (\hbar/eB)^{1/2}$ is the magnetic length and $\gamma = (a^*/l)^2 \sim B$.¹⁶ Thus $a_{\parallel}^* a_{\perp}^{*2} = 4a^{*3}/\gamma \ln\gamma$ and decreases as B is raised. Expressing b in Eqs. (1)–(3) in units of $a_{\parallel}^* a_{\perp}^{*2}$, that is $b^3 = Ma_{\parallel}^* a_{\perp}^{*2}$, in the strong-field limit ($\gamma \gg 1$), and using $h = 1$ we obtain

$$R_H(B) = \frac{1}{en_{\text{eff}}(B)} = \frac{1 - \epsilon(B)}{e[n - \Delta n(B)]}. \quad (4)$$

M is a dimensionless parameter; within our model if a donor does not have a neighbor in the volume $4\pi Ma_{\parallel}^* a_{\perp}^{*2}/3$, it does not participate in electrical conduction at $T \rightarrow 0$.

Figure 2 also shows a fit based on Eq. (4) with M used as a fitting parameter. The theoretical curve shown has $M = 12$; this means that the microscopic MI transition criterion (on the few-donors scale) is $na_{\parallel}^* a_{\perp}^{*2} \approx 3/4\pi M = 0.27^3$, in contrast to the macroscopic (on the whole-crystal scale) Mott criterion $na_{\parallel}^* a_{\perp}^{*2} \approx 0.30^3$.⁹ This difference of the microscopic and the macroscopic Mott criteria is consistent with the picture of the macroscopic MI transition in crystalline semiconductors being a percolation threshold of formation of the infinite metallic donor cluster. The calculated curve in Fig. 2 extends to the magnetic fields above the MI transition although, obviously, our model does not apply in this field range.

Figure 3 shows the $R_H(B)$ data for several other $\text{Hg}_{1-x}\text{Cd}_x\text{Te}$ samples as well as for an InSb sample ($n = 2.2 \times 10^{15} \text{ cm}^{-3}$, $m^* = 0.014m_e$, $\kappa = 16$). The horizontal axis is $\gamma \ln\gamma/na^{*3}$ in order to scale the data for

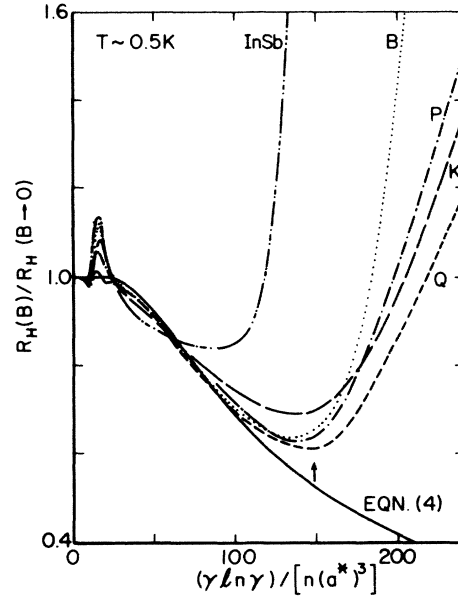


FIG. 3. The normalized Hall coefficients of several $\text{Hg}_{0.79}\text{Cd}_{0.21}\text{Te}$ samples and an InSb sample ($n = 2.2 \times 10^{15} \text{ cm}^{-3}$) vs $\gamma \ln\gamma/na^{*3}$. Sample K has $n = 2.7 \times 10^{14} \text{ cm}^{-3}$, sample B has $n = 1.2 \times 10^{15} \text{ cm}^{-3}$, sample Q has $n = 1.8 \times 10^{15} \text{ cm}^{-3}$, and sample P is the sample of Figs. 1 and 2 ($n = 5.4 \times 10^{14} \text{ cm}^{-3}$). The fit of Eq. (4) is with the same parameter $M = 12$ as in Fig. 2. The arrow indicates MI transition according to the condition $na_{\parallel}^* a_{\perp}^{*2} = 0.30^3$ (cf. Ref. 9).

different samples in accordance with Eq. (4) in the region of strong fields. The scatter of the experimental curves is on the order of the accuracy with which the samples' parameters (n, m^*, κ) are known. The common fit of Eq. (4) is the same as in Fig. 2 ($M = 12$). We note here that for the InSb sample B_{MI} corresponds to $\gamma \approx 20$; therefore, the high-field limit is not fully applicable. This is probably the cause of the worse scaling of InSb data in Fig. 3.¹⁷

The reasonable scaling of the Hall data for the HgCdTe samples with n spanning an order of magnitude is in itself evidence for the impurity-band nature of the conduction near the MI transition (the scaling involves the shallow-donor effective Bohr radius). Our model does not take into account several factors which may play an important role in the electrical transport near the MI transition. We neglected the influence of compensation (except as mentioned in Ref. 4), the effects of finite temperatures, and the electron-electron interaction.¹⁸ The calculation does not take into account the presence of isolated donor doublets and more complex clusters. Also, we spherically averaged the donor distribution although the magnetic field reduces the symmetry to only cylindrical. The geometrical factor h most likely deviates noticeably from the value of 1 that we used (especially,

close to the MI transition), thus increasing $R_H(B)$ and producing the rounding at fields close to B_{MI} as is evident in experimental curves.¹⁹

We believe that our model explains the presence, the direction, and the magnitude of the "Hall dip." A more accurate and involved calculation would produce qualitatively similar results, probably leading to an increased value of M since it would take into account more complex isolated donor clusters. We consider the general agreement of Eq. (4), derived within a very simple model, and the experiment as encouraging and strong evidence for the appropriateness of the tight-binding approach to the impurity-band problem in crystalline semiconductors.

The $Hg_{1-x}Cd_xTe$ samples were supplied by D. A. Nelson of the Honeywell Electro-Optics Division. Part of this work was performed while the authors were guest scientists at the Francis Bitter National Magnet Laboratory, which is supported at the Massachusetts Institute of Technology by the National Science Foundation. We thank P. M. Tedrow, L. Rubin, B. Brandt, and the staff of the National Magnet Laboratory for technical assistance. One of us (V.J.G.) acknowledges support by the U.S. Army Research Office under Grant No. DAAG29-85-K-0098, and one of us (M.S.) acknowledges support by the National Science Foundation through a Presidential Young Investigator Award (Grant No. ECS-8553110).

¹See, e.g., N. F. Mott and E. A. Davis, *Electronic Properties of Non-Crystalline Materials* (Clarendon, Oxford, 1979), 2nd ed.

²*Localization, Interaction, and Transport Phenomena*, edited by B. Kramer, G. Bergman, and Y. Bruynseraede (Springer-Verlag, Berlin, 1985).

³N. F. Mott, *J. Phys. (Paris)*, Colloq. **37**, C4-303 (1976); P. W. Anderson, *J. Phys. (Paris)*, Colloq. **37**, C4-340 (1976); D. J. Thouless, *J. Phys. (Paris)*, Colloq. **37**, C4-349 (1976).

⁴B. I. Shklovskii and A. L. Efros, *Electronic Properties of Doped Semiconductors* (Springer-Verlag, New York, 1984).

We limit ourselves here to the most frequently experimentally encountered situation of moderate compensation K , as opposed to the cases $K \ll 1$ or $1 - K \ll 1$, when ionized impurity potential fluctuations on the length of $(Kn)^{1/3}$ or $[(1 - K)n]^{1/3}$, respectively, play an important role.

⁵That is, the off-diagonal, rather than diagonal, disorder dominates.

⁶F. Kuchar, E. Fantner, and G. Bauer, *J. Phys. C* **10**, 3577 (1977).

⁷V. J. Goldman, H. D. Drew, M. Shayegan, and D. A. Nelson, *Phys. Rev. Lett.* **56**, 968 (1986).

⁸V. J. Goldman and H. D. Drew, *Phys. Rev. B* **32**, 5543 (1985).

⁹M. Shayegan, H. D. Drew, D. A. Nelson, and P. M. Tedrow, *Phys. Rev. B* **31**, 6123 (1985).

¹⁰M. Shayegan, V. J. Goldman, H. D. Drew, D. A. Nelson, and P. M. Tedrow, *Phys. Rev. B* **32**, 6952 (1985).

¹¹D. F. Holcomb and J. J. Rehr, *Phys. Rev.* **183**, 773 (1969).

¹²That is, it does not appreciably participate in the charge transport, although it may not be strictly localized according to P. W. Anderson, *Phys. Rev.* **109**, 1492 (1958) [cf. V. G. Karpov, A. Ya. Shik, and B. I. Shklovskii, *Fiz. Tekh. Poluprovodn.* **16**, 1406 (1982) [*Sov. Phys. Semicond.* **16**, 901 (1982)]].

¹³H. J. Juretschke, R. Landauer, and J. A. Swanson, *J. Appl. Phys.* **27**, 838 (1956).

¹⁴M. H. Cohen and J. Jortner, *Phys. Rev. Lett.* **30**, 696 (1973).

¹⁵Cf. R. E. Prange, *Phys. Rev. B* **23**, 4802 (1981).

¹⁶Y. Yafet, R. W. Keyes, and E. N. Adams, *J. Phys. Chem. Solids* **1**, 137 (1956); B. I. Shklovskii, *Fiz. Tekh. Poluprovodn.* **6**, 1197 (1972) [*Sov. Phys. Semicond.* **6**, 1053 (1973)]; also, Ref. 4, Chap. 7.

¹⁷Both a_{\perp}^* and a_{\parallel}^* are smaller than the corresponding strong-field expressions $2l$ and $a^*/\ln\gamma$ (Ref. 16). At $\gamma = 20$ the discrepancies are about 10% which leads to $a_{\perp}^* a_{\parallel}^*$ smaller than $a^{*3}/\gamma \ln\gamma$ by 30%; that is, a $\gamma = 20$ datum point is shifted by 30% to the left because of the use of the strong-field limit approximation.

¹⁸M. Pollak and M. Ortuno, in *Electron-Electron Interactions in Disordered Systems*, edited by A. L. Efros and M. Pollak (Elsevier Science Publishers B.V., Amsterdam, 1985), p. 287.

¹⁹The factor h is greater than 1 and increases as the MI transition is approached (Refs. 13 and 14).